Proceedings of
2004 ASME/STLE International Joint Tribology Conference
Long Beach, California USA, October 24-27, 2004

TRIB2004-64349

HEIGHT- DEPENDENT ASPERITY RADII OF CURVATURES IN A CONTACT AND FRICTION MODEL

George G. Adams
Mechanical and Industrial Engineering Department
Northeastern University, Boston MA 02115
Email: adams@neu.edu

Sinan Müftü
Mechanical and Industrial Engineering Department
Northeastern University, Boston MA 02115
Email: smuftu@coe.neu.edu

ABSTRACT

The effect of a height-dependent asperity radius of curvature is accounted for in a recently developed scale-dependent model of contact and friction. The contact and friction model includes the effects of adhesion, using the Maugis model, and of scale-dependent friction, using the Hurtado and Kim single asperity friction model. This multi-asperity model has been modified to include the effect of non-contacting asperities. The results indicate the types of conditions under which the effects of a height-dependent asperity radius of curvature affects friction.

INTRODUCTION

Contact and friction affect the operation of many machines and tools that we use every day, as well as some of the most basic activities in nature. Examples range from belt drives, brakes, tires, and clutches in automobiles and in other machines; gears, bearings and seals in a variety of mechanical systems; electrical contacts in motors; slider-disk interactions in a computer disk drive; various MEMS devices; a robotic manipulator joint; the motion of a human knee-joint (natural or artificial); and walking/running.

The friction force F is the tangential force resisting the relative motion of two surfaces which are pressed against each other with a normal force P. Amontons, in 1699, and Coulomb in 1785, developed our phenomenological understanding of *dry* friction between two contacting bodies. Amontons-Coulomb friction states that the ratio of the friction force (during sliding) to the normal force is a constant called the coefficient of *kinetic* friction. Similarly the coefficient of *static* friction is the ratio of the maximum friction force F that the surfaces can sustain, without relative motion, to the normal force. These friction laws can be summarized by defining the coefficient of friction μ as

$$\mu = \frac{F}{P} \tag{1}$$

without distinguishing between static and low-speed sliding friction. Although Eq. (1) provides an extraordinarily simple *phenomenological* friction law, the *nature* of the friction force is not well-understood.

Contact modeling is an essential part of any friction model. It consists of two related steps. First, the equations representing the contact of a single pair of asperities are determined. For nanometer scale contacts the effect of adhesion on the contact area is important. Second, the cumulative effect of individual asperity contacts is determined. Such contact models are uncoupled and represent surface roughness as a set of asperities, often with statistically distributed parameters. The effect of each individual asperity contact is local and considered separately from the other asperities; the cumulative effect is the sum of the actions of the individual asperities (e.g. the well-known Greenwood and Williamson model, [1]).

For sufficiently small size contacts, the adhesion forces between the surfaces affect the contact conditions. Various adhesion models, typically between an elastic sphere and a flat, have been introduced. The model by Johnson, Kendall and Roberts (JKR) assumes that the attractive intermolecular surface forces cause elastic deformation beyond that predicted by the Hertz theory, thereby producing a subsequent increase of the contact area [2]. The model by Derjaguin, Muller and Toporov (DMT), on the other hand, accounts for the adhesive stress outside of the contact area, but assumes that the contact stress profile remains the same as in the Hertz theory [3]. Due to the assumptions involved, the JKR/DMT models are most suitable when the range of surface forces is small/large

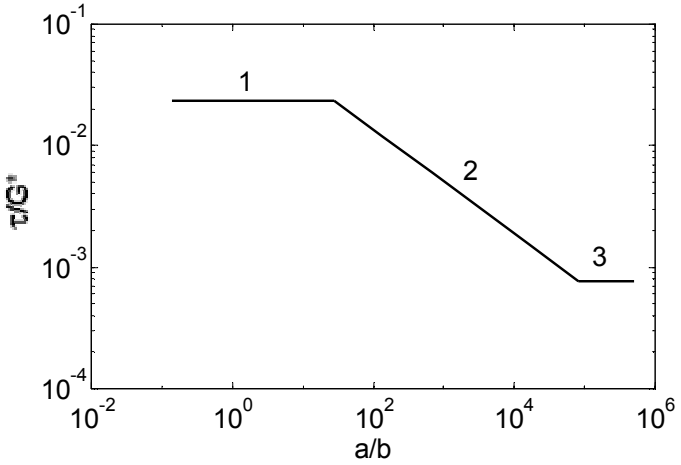

Figure 1. Relationship between friction stress and contact radius according to HK model.

compared to the elastic deformations, as pointed out by Tabor [4]. Another model, introduced by Maugis [5], describes a continuous transition between the JKR and DMT models.

Contact and friction models which deal with adhesion in multi-asperity contacts have also been developed. In the first of a series of papers Chang, Etsion and Bogy (CEB) [6] developed an elastic-plastic multi-asperity contact model for normal loading based on volume conservation of a plastically deformed asperity control volume. In [7], the effect of adhesion was included by using the DMT model for contacting asperities and the Lennard-Jones potential between non-contacting asperities. Finally a model for calculating the coefficient of friction was given in [8]. It assumed that once plastic yielding is initiated in a pair of contacting asperities, no further tangential force can be sustained. Fuller and Tabor [9] developed a theoretical model which used the JKR model of adhesion along with a Gaussian distribution of asperity heights was developed.

Stanley, Etsion and Bogy (SEB) [10] developed a model for the adhesion of two rough surfaces, affected by sub-boundary layer lubrication, in an elastic-plastic multi-asperity contact. Polycarpou and Etsion [11] used the SEB model to predict the static friction coefficient. The tangential load was found using the same procedure as in the CEB model [8] for solid-solid contact. Kogut and Etsion developed multi-asperity contact [12] and friction models [13] which included the effects of plastic deformation. The maximum shear load that an asperity can sustain is limited by the combined normal and shear load which causes the plastic deformation zone to reach the surface. Thus the friction analysis [13] predicts higher friction than the related work in [8]. Yu, Pergande, and Polycarpou [14] extended the CEB model to include an asymmetric distribution of asperity heights.

Experiments in the low and high normal load regimes have shown that *the friction coefficient depends on the magnitude of the normal force*. In particular, these experiments have shown that μ increases with decreasing normal load (Rabinowicz and Kaymaram [15]; Etsion and Amit, [16]).

The scale-dependence of the friction stress for single asperity contacts has recently been investigated by Hurtado and Kim (HK), [17,18]. They presented a micromechanical dislocation model of frictional slip between two asperities for a wide range of contact radii. According to the HK model, if the contact radius "*a*" is smaller than a critical value, the asperities slide past each other in a concurrent slip process where the adhesive forces are responsible for the shear stress; hence the shear stress remains at a high constant value. On the other hand, if the contact radius is greater than that critical value, the shear stress decreases for increasing values of contact radius until it reaches a second constant, but lower value. The relationship between the non-dimensional friction stress ($\bar{\tau} = \tau / G^*$) and the non-dimensional contact radius ($\bar{a} = a/b$) is approximated in Fig. 1. The contact radius "*a*" is normalized by the Burgers vector *b* and the friction stress τ is normalized by the effective shear modulus $G^*=2G_1G_2/(G_1+G_2)$ where G_1 and G_2 are the shear moduli of the contacting bodies. Adams, Müftü, and Mohd Azhar (AMM), [19] incorporated the HK model and the adhesion contact model of Maugis, into a statistical multi-asperity model for contact and friction. The relationship between the friction force and the normal load between two rough surfaces during a slip process was determined. *Three key dimensionless parameters* representing the surface roughness, the friction regime of the contacts, and the surface energy of adhesion, were seen to influence the value of the friction coefficient. In [20], Adams and Müftü included the effect of an asymmetric distribution of asperity heights using a Weibull function to account for skew and kurtosis.

In this paper the effect of a height-dependent asperity radius of curvature on the AMM scale-dependent contact and friction model [19] is determined. Such height-dependence is likely to occur in, for example, polishing operations in which higher asperities are polished to a greater extent and therefore have larger radii of curvature than do the shorter asperities. On the other hand, from the point-of-view of a random surface profile, Whitehouse and Archard [21] found that higher asperities have smaller curvatures. This result is a consequence of the assumed randomness of a surface in which the neighboring points about a *high* peak are more likely to have a height which deviates from the peak height by a greater amount than would the points nearby a lower peak. Extending the work of [21], Onions and Archard [22] found that such a distribution of asperity curvatures increases the contact pressures making plastic deformation more likely to occur. Rather than obtaining and analyzing data for a variety of surface finishes, in this paper we investigate the degree of height-dependence needed to significantly influence friction. It is also noted that modern manufacturing techniques allow a greater degree of control over surface topography than existed at earlier times. In addition, the AMM model [19] has been modified to account for the effect of non-contacting asperities.

DEVELOPMENT OF THE MODEL

Contact Model

The scale-dependent multi-asperity contact and friction model developed by Adams, Müftü, and Mohd Azhar [19] will be extended to include a height-dependent asperity radius of curvature. For two real surfaces separated by a distance *d* (defined from the mean of asperity heights) the number of contacting asperities *n* is

$$n = N \int_{\bar{d}}^{\infty} \bar{\phi}(\bar{z}) d\bar{z} \tag{2}$$

where N is the total number of asperities, σ is the standard deviation of asperity peak heights, $\bar{z} = z/\sigma$ is the dimensionless height coordinate measured from the mean of asperity heights, $\bar{\phi}(\bar{z})$ is the probability density of asperity peaks, and $\bar{d} = d/\sigma$ is the non-dimensional separation between the two surfaces (Fig. 2).

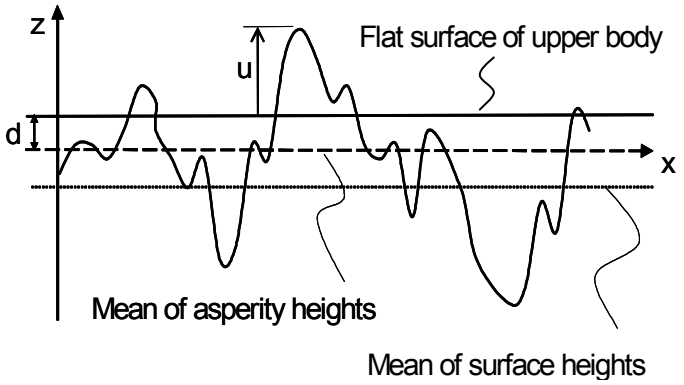

Figure 2. Contact of a rough surface (lower body) with a flat surface (upper body).

The height-dependent radius of curvature is assumed to be in the form

$$r = Rg(\bar{z}), \quad g(\bar{z}) = 1 + \varepsilon \tanh(\rho \bar{z}) \tag{3}$$

where R is the average radius of curvature. The choice of the function $g(\bar{z})$ is somewhat arbitrarily chosen so that the asperity radius of curvature varies smoothly between $R(1-\varepsilon)$ and $R(1+\varepsilon)$. For positive ε higher asperities have greater radii whereas for negative ε the higher asperities have smaller radii. For large ρ the variation in radius with $\bar{z}$ occurs most abruptly in a small region surrounding the average asperity height, whereas for small ρ the variation is more gradual. Although a variety of surface height distributions may be considered, a Gaussian distribution of asperity peaks, which gives the following probability density function, is chosen, i.e.

$$\phi(\bar{z}) = \frac{1}{(2\pi)^{1/2}} \exp\left(-\bar{z}^2/2\right) \tag{4}$$

The relation between the normal load P and deformation $u = z - d$ of two contacting spherical asperities with adhesion is given by the Maugis model [5]. In that model, a uniform tensile stress σ_0 exists between the contacting asperities just outside the contact zone, $a \le r \le c$, where c is the radial extent of the adhesion zone. The separation between the two surfaces at $r = c$ is equal to the prescribed maximum adhesion distance h. Thus the work of adhesion is given by $w = \sigma_0 h$. In [5] the following non-dimensional relations among the asperity contact radius $(\bar{a} = a/b)$, the asperity contact force $(\bar{P} = P/Gb^2)$, and the asperity deformation $(\bar{u} = u/\sigma)$ were obtained

$$\frac{\alpha b}{\pi\beta h g(\bar{z})}\left[\sqrt{m^2-1} + \left(m^2-2\right)\tan^{-1}\sqrt{m^2-1}\right]\bar{a}^2 + \frac{4\gamma b^2}{\pi h^2}\left[\left(m^2-1\right)\tan^{-1}\sqrt{m^2-1} - m + 1\right]\bar{a} - 1 = 0 \tag{5}$$

$$\bar{P} = \frac{8\alpha}{3\beta(1-\nu)g(\bar{z})}\bar{a}^3 - \frac{4\gamma b}{h(1-\nu)}\left[\sqrt{m^2-1} + m^2\tan^{-1}\sqrt{m^2-1}\right]\bar{a}^2 \tag{6}$$

$$\bar{u} = \bar{z} - \bar{d} = \frac{1}{\beta^2 g(\bar{z})}\bar{a}^2 - \frac{2\gamma b}{\alpha\beta h}\sqrt{m^2-1}\,\bar{a} \tag{7}$$

where m is the non-dimensional adhesion radius given by

$$m = \frac{c}{a}, \qquad \lambda = \left(\frac{b}{h}\right)\left(\frac{9\beta\gamma^2}{2\pi\alpha}\right)^{1/3} \tag{8}$$

in which λ is the non-dimensional Maugis adhesion parameter.

In (5)-(7) there are three key parameters α, β and γ which are defined by

$$\alpha = \left(\frac{\sigma}{R}\right)^{1/2}, \quad \beta = \frac{(R\sigma)^{1/2}}{b}, \quad \gamma = \frac{w}{E^* b}. \tag{9}$$

A physical interpretation of the surface parameters α and β is provided by noting that in a simple vertical scaling of the surface by a factor k, the standard deviation of asperity heights σ is scaled by k but the asperity radius of curvature R is scaled by $1/k$. Thus, α is scaled by k, but β remains constant. Hence α is a representation of the surface roughness, and is referred to as the *surface roughness parameter*. The parameter β describes the ratio of the contact radius (due to an asperity penetration equal to σ) to the Burgers vector length. Thus small β are expected to be indicative of nano-scale asperity contacts and progressively larger values of β correspond to transition and larger values of the contact radius (Fig. 2). Therefore β is referred to as the *friction regime parameter*. The *surface energy parameter* γ represents the ratio of the adhesive stress to the product of the composite Young's modulus and the Burgers vector.

It is further noted that for the case considered here, in which one of the surfaces is assumed to be rigid and flat, $G^*=2G$ and the composite Young's modulus is given by $E^* = E/(1-\nu^2)$. Furthermore the relation $G=E/2(1+\nu)$ has been used.

The simultaneous solution of Eqs. (5)-(7) gives the relations among m, $\bar{P}$, $\bar{a}$, and $\bar{u}$ for given values of the surface roughness parameter α, the friction regime parameter β,

the surface energy of adhesion parameter γ, the ratio (b/h), the Poisson's ratio (ν), and the height-dependent radius parameters (ε,ρ).

An expression for the total non-dimensional normal force acting on the nominal contact area is obtained by integrating the normal force on individual asperities, resulting in the total normal force ($\overline{P}_T$)

$$\overline{P}_T = N\int_{\overline{d}}^{\infty}\overline{P}\,\overline{\phi}(\overline{z})d\overline{z} \tag{10}$$

It is noted that due to adhesion during the unloading process, asperities may remain in contact even if the asperity overlap u is negative. This effect has been included in the evaluation of the integrals in Eqs. (2) and (10) by varying the adhesion radius ratio m in Eqs. (5)-(7) when evaluating the force and contact area. Thus the lower limits of the integrals in Eqs. (2) and (10) are effectively slightly less than $\overline{d}$. However, when an asperity breaks free of its mating surface during unloading, its undeformed location may still bring it within the distance h in which there are attractive forces using the Maugis model of adhesion. The effect of these attractive forces on the applied normal force was neglected in [19]-[20], but are accounted for here.

Consider an elastic sphere in close proximity to an elastic half-space. If the minimum separation distance is greater than the adhesion distance h, then the interaction force vanishes. However if the separation distance is less than h, a uniform tensile stress of magnitude σ_0 acts in a circular area of radius c. The surface normal elastic displacement in the center and along the periphery of the circle of interaction for such a loading are given in [23] by

$$u_0 = \frac{2\sigma_0 c}{E^*}, \quad u_C = \frac{4\sigma_0 c}{\pi E^*} \tag{11}$$

respectively. At $r = c$, the separation after deformation must be equal to the adhesion separation (h) resulting in

$$\frac{c}{R} = \left(\frac{4\sigma_0}{\pi E^*}\right) + \sqrt{\left(\frac{4\sigma_0}{\pi E^*}\right)^2 + 2\left(\frac{h-\delta}{R}\right)} \tag{12}$$

It is noted, however, that this solution is only valid if the elastic deformation at the center of the circular area is insufficient to bring these bodies into contact. The normal force between the two bodies is given by $P = \pi c^2 \sigma_0$, which becomes

$$\overline{P} = -\frac{64\beta\gamma\lambda^3}{9(1-\nu)\alpha}\left[1+\sqrt{1+\frac{9\pi}{16\lambda^3}(1-\delta/h)}\right]^2 \tag{13}$$

Thus Eq. (10) needs to be modified to account for the forces exerted by non-contacting asperities by including Eq. (13) for values of $\overline{z}$ greater than $-h$ but less than the value of $\overline{z}$ which causes the asperity to separate from the surface. For values of $\lambda > 0.655$, when any asperity separates it will return to its undeformed position which is outside the Maugis range of adhesion. Thus no correction for non-contacting asperities is needed for those cases.

Friction Model

Although adhesion affects the relationship between the normal force and the contact radius, it does not affect the relation between the friction force and contact radius. From Fig. 1, the dimensionless shear stress is a function of the dimensionless contact radius and is approximated by

$$\log(\overline{\tau}) = \begin{cases} \log\overline{\tau}_1, & \overline{a} < \overline{a}_1 \\ M\log\overline{a} + B, & \overline{a}_1 < \overline{a} < \overline{a}_2 \\ \log\overline{\tau}_2, & \overline{a} > \overline{a}_2 \end{cases} \tag{14}$$

where the left and right limits of region-2 are $(\overline{a}_1, \overline{\tau}_1)$ and $(\overline{a}_2, \overline{\tau}_2)$ respectively. The constants of Eq. (14) are given in [19] where M and B are, respectively, the slope and y-intercept of the line in region-2 of the log-log plot of Fig. 1. The friction force F acting on a single asperity can be determined from Eq. (14) by using

$$F = \pi a^2 \tau \quad \text{or} \quad \overline{F} = \pi \overline{a}^2 \overline{\tau} \tag{15}$$

The total shear force F acting on the nominal contact area can be calculated by integrating the shear forces acting on each asperity against the probability density function, i.e.

$$\overline{F}_T = N\int_{\overline{d}}^{\infty}\overline{F}\,\overline{\phi}(\overline{z})d\overline{z} \tag{16}$$

It is noted that for values of the applied tangential force $(\overline{F}_T)$ less than that given by Eq. (16), the distribution of tangential and normal forces among the asperities may cause some asperities to slip while others continue to stick. However when F reaches the value given in Eq. (16) all contacting asperities will slide resulting in global slip.

Thus, the coefficient of friction μ for two real surfaces separated by a distance $\overline{d}$, can be obtained from the ratio of Eqs. (16) and (10), where (10) has been modified to account for non-contacting asperities.

RESULTS AND DISCUSSION

In Fig. 3 is shown the effect of non-contacting asperities on the friction coefficient. For a given applied force, the adhesive force on these asperities serves to increase the contact force and hence increase the contact area and friction force, thereby giving a larger friction coefficient. As discussed previously, for $\lambda > 0.655$ the effect of non-contacting asperities vanishes. Fig. 3 shows results with and without non-contacting asperities for $\alpha = 0.01$, $\gamma = 0.001$, and with $\beta = 1000$ ($\lambda = 0.523$) as well as with $\beta = 500$ ($\lambda = 0.415$). These cases represent the lowest values of λ used in [19]. The maximum effect on the friction coefficient is 2.1% for $\lambda = 0.523$ and 3.8% for $\lambda = 0.415$. As

was explained in the above, this maximum difference corresponds to the smallest applied load.

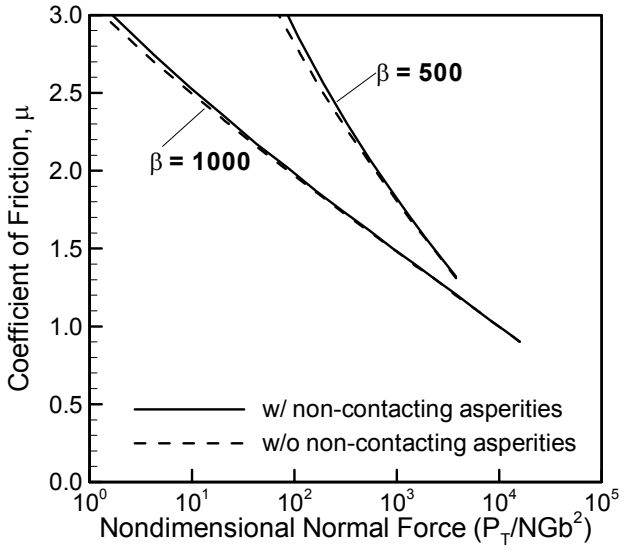

Fig. 3. Effect of non-contacting asperities on the friction coefficient for $\alpha = 0.01$, $\gamma = 0.001$, and with $\beta = 1000$ ($\lambda = 0.523$) and $\beta = 500$ ($\lambda = 0.415$).

Fig. 4 shows the variation of the friction coefficient with the applied force, each for five different values of the parameter ε (1.0, 0.5, 0, -0.5, -0.95) and all with ρ = 0.5. A positive/negative value of ε corresponds to taller asperities which have a greater/smaller radius of curvature than do the shorter ones. For ε = 1.0, the tallest asperities have twice the radius as the average, whereas as for ε = -0.95 the tallest asperities have a radius equal to 0.05 of the average. It is interesting to note that in all three cases shown (Figs. 4a,b,c), an ε of *-0.95* decreases friction and dramatically reduces the load-dependence of friction which was predicted in [19]-[20] for constant radii of curvature. Similarly for ε = 1.0, friction is highest and so is its dependence on normal load. These results occur because for a given normal force, the contact area increases monotonically with the radius of curvature. Thus negative ε give smaller friction than do positive ε. That trend is less pronounced for larger loads in which a greater portion of the asperities are in contact.

CONCLUSIONS

The scale-dependent contact and friction model of Adams, Müftü and Mohd Azhar [19] has been modified in two ways. First the effect of non-contacting asperities was included. This effect was found to be small, mainly because the original model already included the effect of asperities while they remained in contact prior to separation. Secondly the effect of a height-dependent asperity radius of curvature was included. This effect can be significant. For radii of curvature which increase/decrease with height, it was found that the friction coefficient increases/decreases as does its dependence on load.

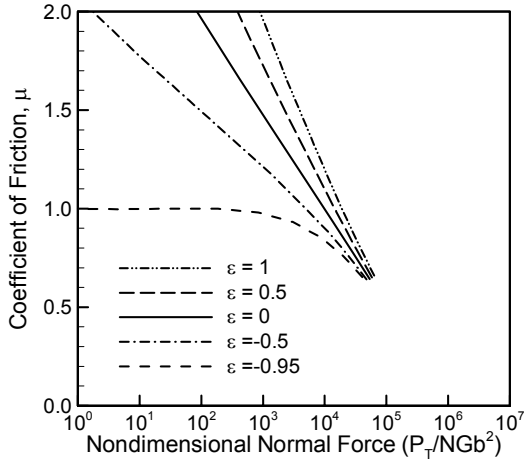

a) $\alpha = 10^{-2}$, $\beta = 10^{3}$, $\gamma = 10^{-3}$, $\rho = 1/2$

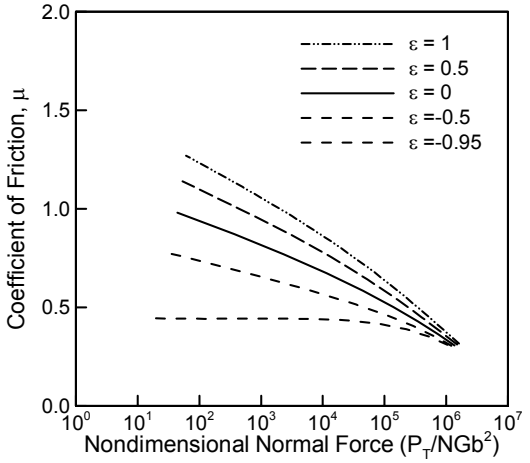

b) $\alpha = 10^{-2}$, $\beta = 5\times10^{3}$, $\gamma = 10^{-3}$, $\rho = 1/2$

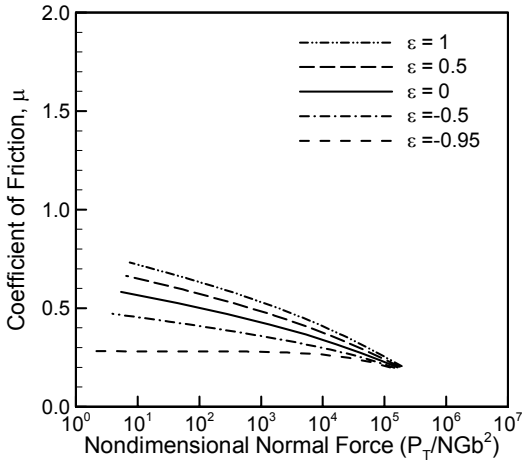

c) $\alpha = 3\times10^{-2}$, $\beta = 10^{3}$, $\gamma = 10^{-3}$, $\rho = 1/2$

Fig. 4a,b,c. The variations of the friction coefficient with applied force, each for five values of the parameter ε and all with ρ = 0.5.

REFERENCES

[1] Greenwood, J.A., and Williamson, J.B.P., 1966, "Contact of Nominally Flat Surfaces," *Proceedings of the Royal Society of London,* **A295**, pp. 300-319.

[2] Johnson, K.L., Kendall, K., and Roberts, A.D., 1971, "Surface Energy and the Contact of Elastic Solids," *Proceedings of the Royal Society of London,* **A324**, pp. 301-313.

[3] Derjaguin, B.V., Muller, V.M., and Toporov, Y.P., 1975, "Effect of Contact Deformations on the Adhesion of Particles," *Journal of Colloid and Interface Science,* **53**, pp. 314-326.

[4] Tabor, D., 1976, "Surface Forces and Surface Interactions," *Journal of Colloid and Interface Science,* **58**, pp. 2-13.

[5] Maugis, D., 1992, "Adhesion of Spheres: The JKR-DMT Transition Using a Dugdale Model," *Journal of Colloid and Interface Science,* **150**, pp. 243-269.

[6] Chang, R.W., Etsion, I., Bogy, D.B., 1987, "An Elastic-Plastic Model for the Contact of Rough Surfaces," *ASME Journal of Tribology,* **109**, pp. 257-263.

[7] Chang, R.W., Etsion, I., Bogy, D.B., 1988, "Adhesion Model for Metallic Rough Surfaces," *ASME Journal of Tribology,* **110**, pp. 50-56.

[8] Chang, R.W., Etsion, I., Bogy, D.B., 1988, "Static Friction Coefficient Model for Metallic Rough Surfaces" *ASME Journal of Tribology,* **110**, pp. 57-63.

[9] Fuller, K.N.G and Tabor, D., 1975, "The Effect of Surface Roughness on the Adhesion of Elastic Solids," *Proceedings of the Royal Society of London,* **A345**, pp. 327-342.

[10] Stanley, H.M., Etsion, I. and Bogy, D.B., 1990, "Adhesion of Contacting Rough Surfaces in the Presence of Sub-Boundary Lubrication," *ASME Journal of Tribology,* **112**, pp. 98-104.

[11] Polycarpou, A.A., and Etsion, I., 1998, "Static Friction of Contacting Real Surfaces in the Presence of Sub-Boundary Lubrication," *ASME Journal of Tribology,* **120**, pp. 296-303.

[12] Kogut, L., and Etsion, I., 2003, "A Finite Element Based Elastic-Plastic Model for the Contact of Rough Surfaces," *Tribology Transactions,* **46**, pp. 383-390.

[13] Kogut, L., and Etsion, I., 2003, "A Static Friction Model for Elastic-Plastic Contacting Rough Surfaces," *ASME Journal of Tribology,* **126**, pp. 34-40.

[14] Yu, N., Pergande, S.R., and Polycarpou, A.A., 2004, "Static Friction Model for Rough Surfaces With Asymmetric Distribution of Asperity Heights," *ASME Journal of Tribology,***126**, pp. 626-629.

[15] Rabinowicz, E., and Kaymaram, F., 1991, "On the Mechanism of Failure of Particulate Rigid Disks," *Tribology Transactions,* **34**, pp. 618-622.

[16] Etsion, I., and Amit, M., 1993, "The effect of small normal loads on the static friction coefficient for very smooth surfaces," *Journal of Tribology*, **115**, pp. 406-410.

[17] Hurtado, J.A,. and Kim, K.-S., 1999, "Scale Effects in Friction of Single Asperity Contacts: Part I; From Concurrent Slip to Single-Dislocation-Assisted Slip," *Proceedings of the Royal Society of London,* **A455**, pp. 3363-3384.

[18] Hurtado, J.A., and Kim, K.-S.,1999, "Scale Effects in Friction in Single Asperity Contacts: Part II; Multiple-Dislocation-Cooperated Slip," *Proceedings of the Royal Society of London,* **A455**, pp. 3385-3400.

[19] Adams, G.G., Müftü, S., and Mohd Azhar, N., 2003, "A Scale-Dependent Model for Multi-Asperity Model for Contact and Friction," *ASME Journal of Tribology,* **125**, pp. 700-708.

[20] Adams, G.G., and Müftü, S., 2003, "Asymmetric Asperity Height Distributions in a Scale-Dependent Model for Contact and Friction," *Proceedings of 2003 STLE/ASME Joint International Tribology Conference,* Pointe Vedra Beach, Florida, October 2003, paper 2003TRIB-258 on CD-ROM.

[21] Whitehouse, D.J., and Archard, J.F., 1970, "The Properties of Random Surfaces of Significance in Their Contact," *Proceedings of the Royal Society of London,* **A 316**, pp. 97-121.

[22] Onions, R.A and Archard, J.F., 1972, "The Contact of Surfaces Having a Random Structure," *Journal of Physics D: Applied Physics*, **6**, pp. 289-304.

[23] Johnson, K.L., 1985, *Contact Mechanics,* Cambridge University Press, Cambridge, United Kingdom.